ABSTRACT

RAJKUMAR, RISHIVANTH. Kirigami Patterned Organic Solar Cell Optimization for Tunable Transmission and Power Conversion Efficiency. Under the direction of Dr. Brendan T. O'Connor).

Semitransparent solar cells have opportunities for implementation in building windows and in agriculture applications. These applications would broaden the installation opportunities of solar energy increasing the production of renewable energy. However, semitransparent solar cells typically have a static transmittance that cannot be dynamically adjusted to meet the illumination requirements of a particular application. Ideally, one could vary the transmittance over time similar to window blinds in buildings and shade cloths in greenhouses. For example, in greenhouses it is necessary to adjust the transmittance level during the day and season, which is currently achieved using shade cloths. These shade cloths block incoming light, usually without spectral selection and the reflected sunlight is not utilized. Replacing shade cloths with solar cells could potentially act as a light management system for the greenhouse while harnessing the energy of the undesired sunlight.

Thus, this thesis explores the opportunity of designing a Kirigami-inspired semitransparent organic solar module that has controllable transmittance. The art of Kirigami is one that uses cuts and folds in sheets to vary shapes and patterns with the application of strain. Here, we employ a Kirigami cut pattern that opens the solar module with applied strain to increase transmittance through the module. We employ organic solar cells due to there thin and flexible nature. They can be integrated into a Kirigami cut patterned surface with relatively simple fabrication and remain function with bending under an applied strain. Organic solar cells also have well-defined spectral absorption characteristics making them attractive for semitransparent applications that would benefit from spectrally varied transmittance.

In this work, Kirigami inspired organic solar cells are modelled using a combination of finite element analysis (FEA), transfer matrix optical modeling, image processing, and analytical geometry analysis. The Kirigami cuts impart stretchability to flexible substrates by opening the cuts and buckling the substrate as it is strained. The cut pattern design was varied to determine the impact of the pattern on transmittance and power conversion efficiency (PCE) with applied strain. We use FEA to capture the transmittance of the cells with strain. The stress distribution of the modules under various stretch conditions were also simulated and examined to ensure that the cells would not fail. In addition, analytical models were developed that relate strain to the tilt angle of the OPV cells. Then the output from transfer matrix simulations was used to predict power generation. Combined this modeling provided a comprehensive prediction of performance for the Kirigami-inspired OPV cells.

Modeling shows that transmittance for the Kirigami OPV substrates can vary significantly with angle and strain. At 0 degrees, transmittance is maximum and starts dropping to 80-90% at 30 degrees, 50-70% at 60 degrees, and as low as 10-30% as the angle approaches 90 degrees. The Light Utilization Efficiency (LUE) was calculated for different Kirigami designs. For the best-performing design (Rx=2, Ry=4), the LUE reached approximately 2.75 at 20% strain. The LUE of the Kirigami OPVs, particularly those with PM6 active layers, shows that these devices can outperform traditional OPVs in terms of LUE, especially at lower strains. This highlights the potential of Kirigami OPVs for applications requiring both high efficiency and tunable transmittance, such as building-integrated photovoltaics and greenhouse integration. The Kirigami cut pattern OPV cells thus hold promise as a strategy to achieve high performance semitransparent solar cells with dynamic transmittance management.

© Copyright 2024 by Rishivanth Rajkumar

All Rights Reserved

Kirigami Patterned Organic Solar Cell Optimization for Tunable Transmission and Power Conversion Efficiency

by
Rishivanth Rajkumar

A thesis submitted to the Graduate Faculty of
North Carolina State University
in partial fulfillment of the requirements for the degree of
Master of Science

Mechanical Engineering

Raleigh, North
Carolina 2024

APPROVED BY:

Dr. Brendan T. O'Connor	Dr. Tarek Echekki
Committee Chair	

Dr. Jie Yin

DEDICATION

To my mother and my extended family.

BIOGRAPHY

Rishivanth was born and raised in Chennai, Tamil Nadu, India. He graduated with a bachelor's degree in mechanical engineering from SASTRA Deemed University, Thanjavur in 2022. Post that, He joined NC State for his MS in Mechanical Engineering where he worked under Dr. Brendan T. O'Connor on Kirigami structures.

ACKNOWLEDGMENTS

From the bottom of my heart, I am grateful to Dr. Brendan O'Connor for all of his help, support, and knowledge as this thesis came together. His extensive expertise in materials science and renewable energy has greatly influenced the course and caliber of this study. My learning experience has been tremendously enhanced by Dr. O'Connor's persistent support, perceptive criticism, and dedication to academic quality. He has also motivated me to pursue creativity in my work.

His tolerance and readiness to offer helpful and critical feedback have enabled me to overcome many obstacles and improve the goals I have for my research. Under his guidance, I have improved my technical proficiency and developed a more comprehensive comprehension of the wider consequences of my study on sustainable energy solutions.

I would also like to thank Ronnald Booth and Jakob Triemstra for their advice and guidance throughout this work.

TABLE OF CONTENTS

LIST OF FIGURES

Chapter 1: Introduction

1.1. Solar energy and Kirigami patterned substrate

Solar energy is crucial today due to its potential to provide a clean, renewable, and abundant source of power. As concerns about climate change and environmental degradation grow, solar energy offers a sustainable alternative to fossil fuels, reducing greenhouse gas emissions and dependence on non-renewable resources. Additionally, advancements in solar technology have made it more affordable and accessible, enabling broader adoption across various sectors. By harnessing solar energy, we can work towards a more sustainable future, ensuring energy security and supporting global efforts to mitigate climate change.

In the area of photovoltaics, organic photovoltaics (OPVs) are a relatively new technology that are distinguished by their lightweight, flexible, and possibly inexpensive manufacturing. In contrast to conventional silicon-based solar cells, OPVS use polymers or molecules to absorb light and turn it into power. A transparent electrode (often indium tin oxide, or ITO), a hole transport layer, a photoactive layer made up of donor and acceptor materials, and a metal electrode (like aluminum) make up an OPV. Although, some interesting examples of single component OPVs have been explored [1], the current state-of-the art solar technology is based on the 'lattice-matched' GaInP/ GaInAs/Ge solar cell [2]. In semitransparent OPVs, Perovskite-based semitransparent OPVs with PCE of 9.2% and 30% visible light transmittance is considered to be cutting edge [3]. A key factor for OPV materials implementation into industrial relevant devices is their active layer thickness tolerance as solar cell performances are typically reported with thicknesses on the order of 100–150 nm, but thicker films (ca. 300 nm) are needed for printing and roll-

to-roll processing [4]. The organic components in the OPV cell absorb photons and produce electron–hole pairs when light strikes its active layer. In an OPV cell, photons interact with organic semiconducting elements in the cell's active layer to absorb light. Electrical current is produced when a photon that has energy equal to or higher than the material's bandgap energy is absorbed. In order to maximize the conversion of sunlight into electrical power, the materials are engineered to have substantial absorption in this spectral region [5]. PM6 is a well-known and widely researched donor-acceptor polymer in the field of OPVs. PM6 is a polymer with excellent film-forming properties, good charge mobility, and a high absorption coefficient in the visible light spectrum. Y6 is a non-fullerene acceptor that has gained attention due to its strong absorption in the near-infrared region, high electron mobility, and excellent miscibility with donor polymers like PM6. The choice of PM6 in this study is driven by its record-breaking PCEs and stability under various environmental conditions, making it a promising candidate for high-performance OPV cells. Figure 1.1 shows the schematic diagram of OPV for different types of junction structures.

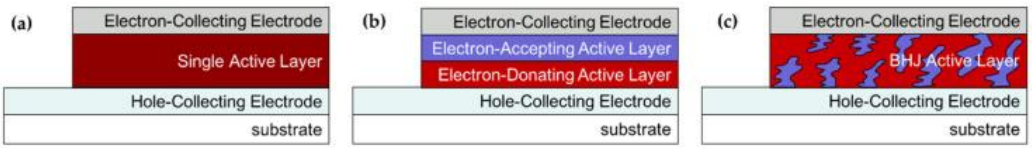

Figure 1.1. Schematic diagram of OPV with (a) single active layer structure, (b) bilayer heterojunction structure, and (c) bulk heterojunction structure, obtained from [6].

OPVs present a promising alternative to traditional silicon-based photovoltaic technology due to their lightweight design, flexibility, and potential for low-cost

production [7]. Uniquely, they can be processed on clear plastic substrates and have a well-defined spectral absorption character that depends on the design of the molecules [8]. These attributes make them particularly suited for semitransparent solar cell applications [9]. For example, absorption of the OPV layer can be pushed into the near infrared improving visible light transmittance [10]. Yet, semitransparency still has limitations based on unavoidable reflection from the cell and absorption of active layer components including the electrodes. In addition, the OPV cells will have a static optical transmission that cannot be varied with time as the lighting needs of an application may change. For example, dynamic lighting needs to balance lighting and overheating in a greenhouse application that may change throughout the day. To achieve dynamic transmittance, this research explores the transformative potential of Kirigami designs to enhance the functionality of OPV cells.

Kirigami, the art of cutting and folding materials to create intricate and functional designs. significant advantages in this context. Its applications span various fields, including medical devices, architecture, robotics, and renewable energy [11]. By leveraging Kirigami designs, it is possible to create medical devices that conform better to the human body, more robust and flexible architectural structures, and compact, efficient robotic systems [12]. In the context of semitransparent solar cells, Kirigami design provides the ability to achieve dynamic transmittance by forming a structure that can open and bend with applied strain to increase optical transmittance. The Kirigami-design is particularly suitable for OPV cells due to the inherent flexibility of OPVs, and the ability to process on plastic substrate that can include cut patterns with relative ease. The primary objective of this research is to investigate the relationship between strain-induced

deflection in Kirigami structures and their overall performance in photovoltaic applications. As Kirigami structures are strained, their surfaces shift orientation, affecting PCE, transmittance, and other output parameters. The study aims to analyze how different cut ratios and design decisions influence these strain-induced changes. To estimate light absorption in organic solar cells, this research employs Transfer Matrix simulations [13].These simulations model how light interacts with the multiple layers of the solar cell, predicting the amount of light absorbed at various angles and wavelengths. By integrating these simulations with geometric modeling of Kirigami structures, the research can estimate power generation under different conditions. This approach helps in understanding the dynamic range of transmittance and the corresponding power generation capabilities of Kirigami-inspired solar panels.

To expand the implementation of solar power into applications such as agrivoltaics, window integration, and wearable power sources there have been several innovative cell designs. Examples of these designs include flexible or lightweight panels. This adaptability is crucial for situations where space may be limited, like in cities or on unusual surfaces. Additionally, well-designed panels can increase public acceptability and deployment opportunities by improving the visual integration into infrastructure and buildings.

Figure 1.2. a) Solar panel attached to the roof of a greenhouse. b) Light transmittance observed inside a greenhouse through the evenly spaced solar panels. c) Greenhouse fitted with a mechanical solar tracking device. d) Panels fitted onto a greenhouse roof, from [14].

1.2. Semitransparency in solar cells

A major development in photovoltaic technology, semitransparency in solar cells offers both practicality and visual appeal [11]. These cutting-edge cells are made to capture solar energy and permit some light to pass through their surfaces. They are perfect for applications where it is important to maintain visibility or incorporate solar power into architectural designs because of their dual capacity. Semitransparent solar cells can be effortlessly integrated into windows, building facades, and even electronic gadgets to harness sunlight efficiently while preserving a certain amount of transparency while not sacrificing their aesthetic appeal. The current state of semitransparent solar cell research is concentrated

on improving performance, robustness, and adaptability for wider uses. One area of innovation is enhancing the transparency of solar cells while keeping or even raising their efficiency of power conversion. To achieve this balance, researchers are experimenting with new materials and manufacturing processes, like thin-film technologies and transparent conductive oxides (TCOs) [12]. Additionally, efforts are being made to improve the stability and longevity of semitransparent solar cells so that they can tolerate environmental conditions including moisture, UV rays, and mechanical stress for extended periods [13].

OPV cells' Light Utilization Efficiency (LUE), which gauges how well the cell turns absorbed light into electrical energy, is a critical factor in assessing the cells' performance. LUE is the product of transmittance and PCE [14]. A higher percentage of incident light being converted into usable electrical power is indicated by a higher LUE, which directly correlates to the OPV device's improved overall performance and efficiency. By increasing OPVs' PCE, optimizing LUE helps to make them more viable for real-world applications and competitive with more established solar technologies.

1.2.1. Kirigami Design

Kirigami, the technique of cutting and folding materials to create functional designs, offers unique advantages over origami, which involves only folding. Although both methods have their roots in traditional Japanese art, Kirigami is especially useful for contemporary engineering and design applications because of its novel use of cuts that enable a wider range of motion and structural alteration [7]. By using Kirigami patterns, it is possible to create solar panels that adjust their transmittance and optimize energy capture, enhancing the efficiency and functionality of solar installations in diverse environments. By examining the capabilities

of Kirigami-inspired solar panels, the study aims to contribute to the development of more efficient and adaptive solar panel design. With its ability to construct lightweight, robust, flexible, and stable structures, Kirigami offers creative answers to difficult engineering problems. For instance, solar panels modeled after Kirigami may track the sun more precisely, improving energy capture and overall efficiency [15]. Figure 1.2 represents the diversity in Kirigami patterns. For this study pattern Figure 1.2(a), with a cut-only brickwork pattern is chosen for its suitability for window applications.

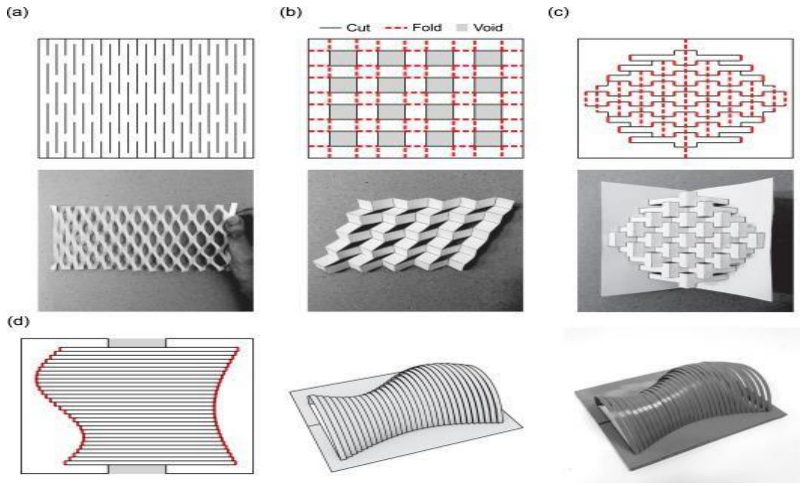

Figure 1.3. Classification of existing and proposed Kirigami patterns based on their motion behavior. a) Cut-only Kirigami, b) Cut-and-fold Kirigami, c) Pop-up Kirigami (top image: 2D Kirigami pattern, bottom image: transformed 3D surface), d) Proposed bending-active active Kirigami (from left to right: 2D pattern, simulated and fabricated 3D surfaces), obtained from [16]

1.2.2. Kirigami in solar panel design

In the context of solar panel design, Kirigami solar structures provide the opportunity to enhance the effectiveness of photovoltaic systems. The ability of Kirigami solar panels to stretch and deform in controlled ways to generate a range of tilting surfaces boosts light absorption throughout the day, in contrast to traditional blinds with solar cells [15]. Additionally, because of their flexibility and versatility, solar panels with Kirigami designs can be used for a wide range of purposes, such as large-scale solar farms, portable solar devices, and urban environments. This is achieved by inserting custom-cut patterns into flexible solar materials for the desired application. This deformation boosts the PCE of the panels by enabling them to track the sun's movement efficiently without the need for large, cumbersome mechanical tracking systems [5]. The lower installation and maintenance costs while simultaneously enhancing the aesthetic appeal provide Kirigami patterned solar panels to be a compelling choice. The Kirigami pattern used in this study can improve both PCE and LUE. The study also elucidates the relation between transmittance and PCE, parameters that are especially useful for applications that need dynamic solar harvesting, like greenhouses or residential settings where the light changes over the day. By allowing solar panels to remain in perfect alignment with the sun, Kirigami designs not only improve energy efficiency and catch more light but also provide structural advantages like decreased material fatigue and increased resistance to mechanical stress. Figure 1.3 shows how the Kirigami cut solar OPV behaves when it opens upon application of strain.

This research aims to advance the design and optimization of Kirigami-patterned organic solar cells by focusing on the following key objectives:

- Design and Optimization: Develop a novel Kirigami-patterned organic solar cell that offers tunable transmittance and enhanced PCE.
- Impact Evaluation: Investigate the influence of various Kirigami cut patterns on the transmittance and PCE of the solar cells when subjected to applied strain, identifying how different patterns respond to mechanical deformation.
- Optimization of Cut Ratios: Determine the optimal cut ratios that strike a balance between maximizing light transmission and achieving high power generation, ensuring the solar cells perform effectively across different applications.
- Design Guidelines: Establish design guidelines for Kirigami-structured OPV systems, with a focus on specific applications such as building-integrated photovoltaics (BIPV) and agricultural greenhouses, where the balance of light transmission and energy generation is crucial.

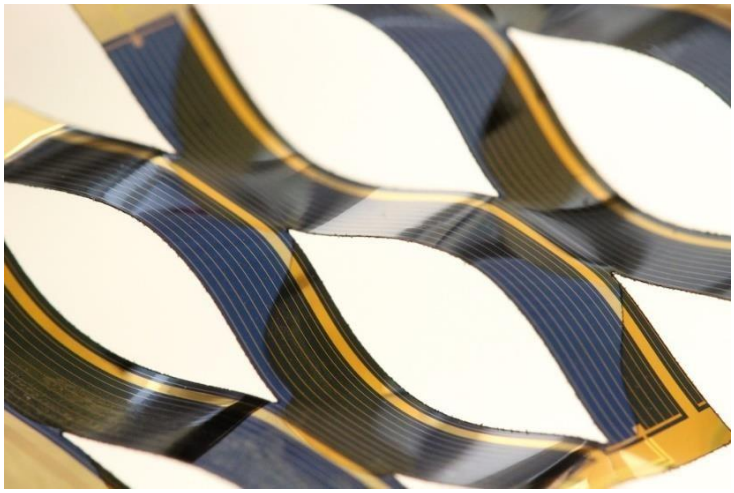

Figure 1.4. Integrated thin-film, crystalline GaAs solar cells, mounted by cold weld bonding on a Kapton carrier substrate, as used for testing. Here, LC=15 mm, x=5 mm and y=5 mm (R1=R2=3), obtained from [15].

Chapter 2: Cut patterns and FEA simulations

When designing Kirigami modules, there are certain parameters to be kept in mind. These include the cut length, the width of the module and the distance between the cuts along the length and widths. These dimensions directly affect the pattern's ability to withstand mechanical stress and strain. Furthermore, they determine the pattern's capacity to deform in a regulated way under different strain conditions and maintain its structural integrity. By modifying these factors, we can customize the Kirigami patterns to fit certain uses, enhancing their effectiveness in domains including flexible electronics, biomedical devices, and deployable structures [17].

The design shown in Figure 2.1 builds upon existing parallel-cut Kirigami patterns but incorporates novel aspects in its application to OPVs and its optimization for both mechanical and optical performance.

Previous studies, such as Lamoureux et al. (2015), explored Kirigami-inspired solar tracking systems using crystalline gallium arsenide (GaAs) cells. However, this study uniquely applies the concept to OPVs, which have different optical and mechanical properties. The specific contributions include:

Application to OPVs: This study is among the first to apply Kirigami patterns to organic solar cells, taking advantage of their flexibility and spectral absorption characteristics.

- Comprehensive modeling approach: Unlike previous works that focused on either mechanical or optical aspects, this research integrates FEA, transfer matrix optical modeling, and analytical geometry analysis. This comprehensive approach allows for simultaneous optimization of mechanical deformation, light transmission, and PCE.

- Cut ratio optimization: The study systematically explores the impact of varying cut ratios on both structural openness and photovoltaic performance. This level of detailed optimization for Kirigami OPVs has not been previously reported.
- Light Utilization Efficiency (LUE) analysis: The research introduces LUE as a metric to evaluate the overall performance of Kirigami OPVs, considering both transmittance and PCE.
- Application-specific design guidelines: The study provides insights into optimizing Kirigami patterns for different applications, such as high-efficiency solar farms or semitransparent building-integrated photovoltaics.

While other researchers have studied similar configurations, they typically focused on single aspects such as the studies done by Rafsanjani and Bertoldi (2017) analyzed the buckling behavior of Kirigami structures but did not consider photovoltaic performance. Similarly, the solar tracking study conducted by Lamoureux et al. (2015) demonstrated solar tracking with Kirigami but used rigid GaAs cells and did not optimize for semitransparency.

This study's novelty lies in its comprehensive approach to optimizing Kirigami OPVs for both mechanical and photovoltaic performance, with a focus on tunable transmittance.

The design of the cut pattern used in this study is a Parallel- cut Kirigami design as shown in Figure 2.1. Parallel-cut Kirigami design offers significant advantages since it creates a predictable and uniform deformation across the panel which allows for precise control over the panels' shape and orientation [18]. The deformation of parallel-cut patterns enables the dynamic orientation of solar panels, optimizing their angle relative to incoming sunlight and significantly improving power output. This design imparts super-stretchability to otherwise inextensible materials, beneficial for flexible organic solar panels that must conform to various

surfaces while maintaining functional integrity. Additionally, parallel-cut Kirigami allows for localized movement and reorientation of specific panel sections, ensuring optimal sunlight exposure throughout the day. By introducing additional degrees of freedom, Kirigami cutting increases mechanical flexibility, enabling solar panels to better withstand mechanical stress and strain, reducing damage risk, and extending lifespan. These features make parallel-cut Kirigami design a promising approach for improving the performance and durability of organic solar panels in dynamic environmental conditions. For the application of window blinds, the area of the windows becomes a constraint in designing the Kirigami solar panel. The model chosen for this study overcomes this constraint to a reasonable extent since the faces of this pattern rotate in place while the total area expansion is not as high as other patterns. Furthermore, this pattern provides a more uniform appeal and closely resembles the blinds in use today. The relationship between the cut length and total length of the segment in the corresponding x and y directions is represented by cut ratios, namely Rx and Ry which are determined by the formulae:

$$Rx = \frac{Lc}{x} \tag{2.1}$$

$$Ry = \frac{Lc}{y} \tag{2.2}$$

Wherein Lc is the cut length of the pattern, x is the distance between the cuts along the horizontal and y is the distance between the cuts along the vertical direction, as shown in Figure 2.2.

The cut ratios determine how crowded the cuts are in each panel. Figure 2.1 is an example of how varying the cut ratios will change the cut patterns on the Kirigami structure. Keeping

the length of the cut (Lc) constant, when we increase the Rx and Ry values, the corresponding x and y values i.e., the distance between the cuts decreases [19]. By controlling these parameters, we can control how crowded the cuts are in the Kirigami model. The closeness of each cut pattern affects how the faces of the panel buckle and that in turn affects the openness of the structure and how robust the module is. The research methodology employs a multi-step approach to analyze and optimize Kirigami-patterned OPVs:

1. SolidWorks is used to create precise 3D models of the Kirigami structures, allowing for systematic variation of cut ratios and dimensions.
2. These models are then imported into ANSYS for FEA to simulate mechanical deformation and stress distribution under applied strain.
3. The deformed geometries from FEA are analyzed using ImageJ to quantify open area and transmittance.
4. Analytical models relating strain to tilt angle are developed to complement the numerical simulations.

This integrated approach comprehensively predicts Kirigami OPV performance under various strain conditions and cut pattern designs.

The modeling details have been discussed in detail in the following sections.

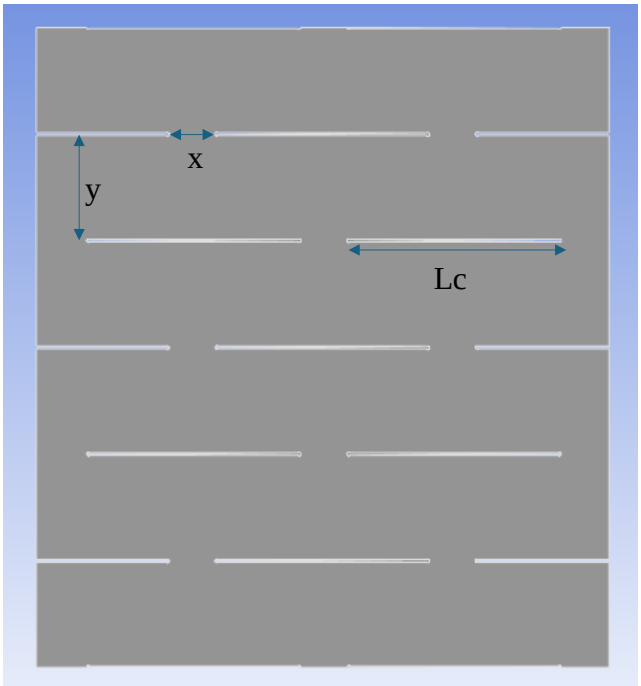

Figure 2.1. SolidWorks model of Kirigami module depicting the cut length of Lc and the distance between the cuts along the length and the width as x and y.

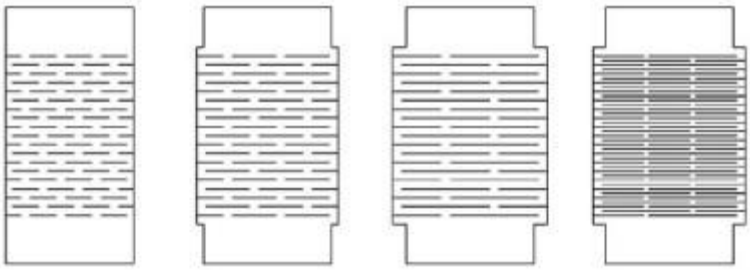

Figure 2.2. Parallel cut Kirigami cut patterns indicate the positioning of cuts for equal Rx and Ry values in the increasing ratios from left to right, obtained from [20].

2.1. Modelling Kirigami cut patterns

The parallel-cut Kirigami structure is modeled using SolidWorks, a CAD software widely used in mechanical design. The length of the module is calculated using the cut length and the cut ratios. Depending on the number of cuts, the length of each cut (Lc), and the distance between the cuts along the horizontal direction (x), the total length of the module was added and set in the dimension parameter. The width of the cut is calculated by multiplying the distance between the cuts along the vertical direction and the distance between the cuts (y). The cut-extrude capability was then used to insert cuts, with the cut length chosen to be 6cm. The cut ratios Rx and Ry were then used to calculate the distances between the cuts i.e., x and y values while keeping the cut length constant. Altering the x and y values while maintaining a constant cut length allows the development of several models with different Rx and Ry values. In this study, the Rx values of 1.5, 2, and 4 were chosen, and for Ry 2, 4, and 6 were chosen. Since the cut ratios specify the distance between the cuts, with the chosen values, the variance in openness and in extension the transmittance is observed. The distance between the cuts along the horizontal axis (x) with a cut length (Lc) of 6 cm varies from 1.5 cm (for Rx = 4) to 4 cm (for Rx = 1.5) and similarly along the vertical axis, the distance between the cuts (y) varies from 1cm (for Ry=6) to 3cm (for Ry=2). The x values are apt for the opening of the pattern, when the distance was greater than 4 cm, the model was stiffer and would require a more blind area to open them, and when they were lesser than 1.5cm, the model was flimsy. The y values were chosen such that the faces would not be too wide to practically mimic the current window blinds in use today. Furthermore, 2 circular holes are provided at the ends of each cut to inhibit crack propagation owing to stress concentration [16].

2.2. FEA Simulation of the modeled Kirigami structure

Researchers have utilized FEA to model the mechanical and optical properties of Kirigami structures under strain. Typically, FEA simulations involve creating detailed meshes of the Kirigami patterns and applying forces or displacements to observe resulting deformations, which are then correlated with optical transmittance properties. In “Piezoelectric strain sensor with high sensitivity and high stretchability based on Kirigami design cutting”, Young-Gyun Kim et al., used Ansys, an FEA software, to conduct stress distribution of PVDF under different strains for parallel-cut Kirigami patterns. It depicts the stretched state of the film as well as the stress value when stretched to the maximum strain depending on the pattern design. Furthermore, they also showed that a longer cut can increase the maximum strain while the smaller margin results in low durability. [21]

This study utilizes similar principles from Kim’s work including the material property considerations and boundary conditions for parallel-cut Kirigami designs for organic solar panels, leveraging FEA modeling to maintain structural integrity while optimizing transmittance and LUE.

The Kirigami model that is created in SolidWorks is imported into Ansys which is an FEA software that allows for mechanical simulations. The material used in the simulation was polyethylene since it provides a good representation of the Kirigami model to be analyzed. For this study, non-linear analysis settings were used to observe the out-of-plane buckling of the faces of the Kirigami module. This setting also ensures that large deformations and material nonlinearity are considered which is more accurate for polyethylene due to its non-linear nature. The whole model is analyzed as shell structure since the thickness is very small

compared to the length and width, and Ansys has the ability to treat the model as a thin structure where thickness is given as a parameter. To observe the opening of the substrate, a displacement boundary condition was applied along one edge while the opposite edge was given a fixed boundary condition. The strain values are varied from 0 to 60 percent with periodic intervals. Through this procedure, we can assess each model's behavior at a given strain percentage, which gives us information about the effectiveness and appropriateness of various Kirigami configurations for the purposes for which they are intended. The stress concentration is also found, depicted in Figure 2.5, to observe where the maximum stress is felt in the substrate allowing for better designs in the future.

Figure 2.3 depicts the openness of the model under different strain values. On the left, the intensity of stress is shown where the most stress is towards the bottom depicted in red. On the right of each simulation, the binary image is shown where the red areas show the openness of the structure. The simulation is carried out for all the cut patterns i.e. for all Rx and Ry ratios under 10%, 20%, 40%, and 60%. The snaps of the model are taken and imported to ImageJ software for a detailed analysis to find the openness area of the substrate. By using this method, the open areas for all the cut patterns under the different strains are recorded and the transmittance is calculated.

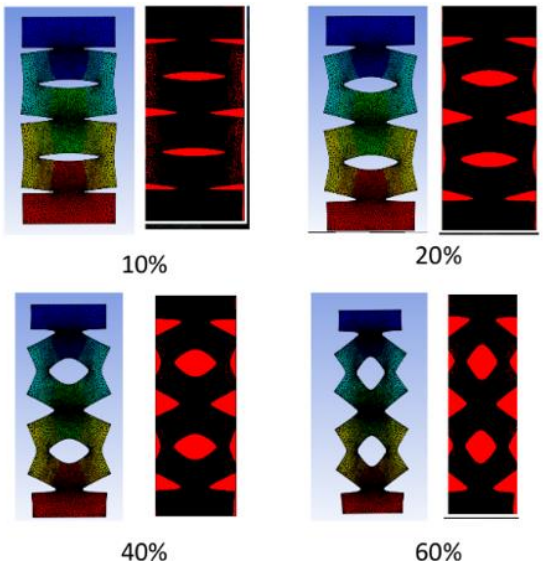

Figure 2.3. FEA simulation for Kirigami structure with strain values of 10%, 20%, 40% and 60%.

The images on the left represent the stress distribution whereas the images on the right are the binary pictures from ImageJ.

In Figure 2.4, the red areas within the module are the openings of the cuts. When we stretch the pattern, the faces lift at an angle while pulling on the edges, this area in red on the left-most and the right-most is also considered since they contribute to the transmittance. The areas are then added to give the total open area. The openness is calculated by dividing the open area by the area of the model before inducing strain. The openness is directly recorded as transmittance and the related graphs for transmittance as a relation of strain is plotted.

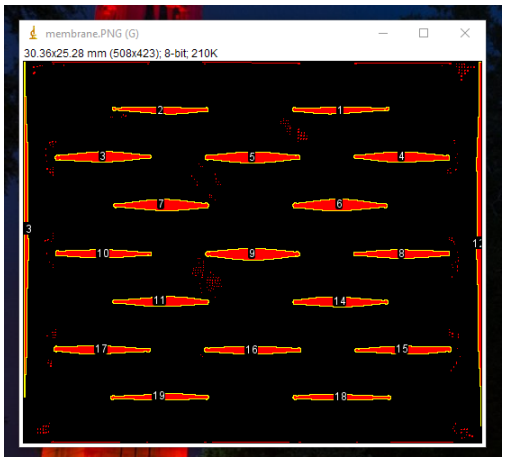

Figure 2.4. Image J analysis of the binary picture of strained Kirigami patterned substrate imported from Ansys where the numbered red areas represent the areas opened due to cuts being strained to 10 percent.

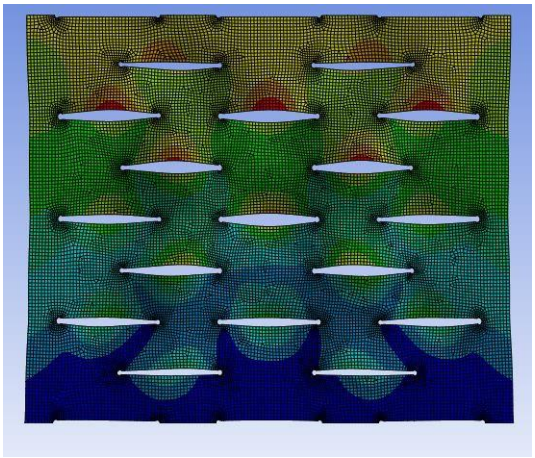

Figure 2.5. FEA Model of the Kirigami substrate that underwent a strain of 10 percent depicting the strain concentration around the cuts and within its boundaries.

2.3. Design parameters

It describes a Kirigami construction modeled in SolidWorks with straight cuts. The axial stretching of the sheet causes controlled buckling in the transverse direction, which causes the feature angle to change synchronously along its length. The integrated thin-film solar cells can track the sun with accuracy because of their special geometric response. The efficiency and macroscopically planar nature of the solar panels are maintained by the Kirigami structure. Dynamic Kirigami structures work by flexing and adjusting their angles in response to applied strain, which maximizes the performance of solar tracking.

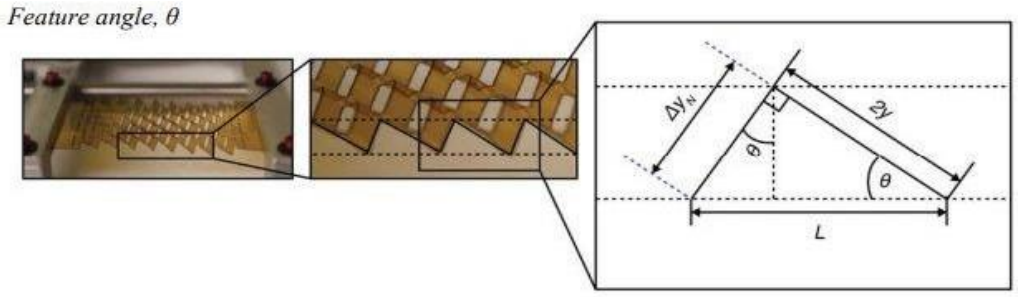

Figure 2.6. A depiction of the face angle of incidence in the strained Kirigami patterned substrate (on the left) and a diagram representing the same on the right were obtained from [15].

A crucial design factor that determines the mechanical flexibility and optical performance of Kirigami solar systems is the cut shape. The flexible substrate has slices that are distinguished by their length and the distance apart from one another. The maximum amount of out-of-plane deformation that the structure can experience when stretched is determined by the length of the cuts. Longer cuts can often withstand more distortion, which makes it possible to vary the feature angles more significantly—an

important factor in designing the Kirigami flexible panel for our application. The material's flexibility is influenced by the breadth of the cuts; smaller cuts typically preserve structural integrity while enabling the required mechanical response. The homogeneity and distribution of strain throughout the structure are influenced by the distance between the cuts. Cuts positioned optimally distribute deformation, avoiding localized stress concentrations that might cause material failure. To maximize the system's overall effectiveness in gathering solar energy, a balance between mechanical robustness and the capacity to dynamically modify the orientation of the embedded solar cells must be struck via the interaction of these geometric characteristics.

2.4. Out of plane tilt

To describe a strained Kirigami model, we can use two featured angles, θ, the front-to-back tilt angle of the surface when looking down the axis of strain, and β, the left-to-right tilt angle of the legs of the Kirigami structure. While the faces of the Kirigami structure are only tilted by θ, the legs are tilted in different directions by θ and β.

The legs of a Kirigami structure that is under stress tilt by an angle of β (yellow vector) in one plane and θ in a perpendicular plane. This tilting alters the angle at which light falling from above (the zenith) impacts the legs, an angle that is essential for determining the angle of the incident light. The dot product (purple vector) of the zenith vector with the normal vector of the tilted leg plane yields this angle of incidence as mentioned in Figure 2.7. To obtain the normal vector for the leg plane, tilt the normal vector of the face plane by θ and β, respectively, making sure the tilt direction is perpendicular to the normal vector. This all-inclusive method makes it possible to precisely model the angle

of incidence, which is crucial for comprehending and optimizing the Kirigami-cut OPV structure's PCE as its transmittance changes with strain.

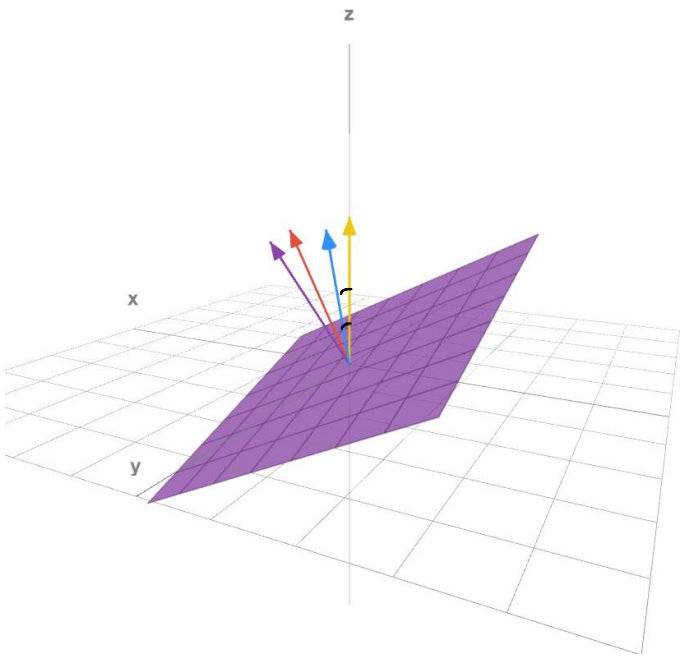

Figure 2.7. Out of plane tilt where the red and blue vectors are tilted by angles θ and β from the unit Zenith (yellow vector) and the purple vector is the resultant of the two tilted by the resultant angles of incidence from the unit zenith.

Chapter 3: Output parameters

3.1. Angles of incidences vs strain

We have multiple output parameters including the face angles, strain, and transmittance which we will discuss below. We will first see the angles of incidences vs strain.

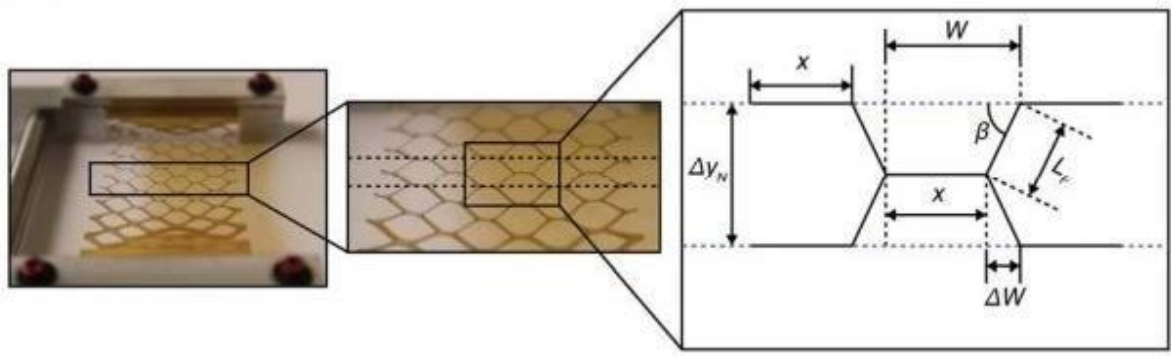

Figure 3.1. Depiction of cut length (x), leg angle of incidence (β), initial width of the cut length with the distance between the cuts (w) and the change in the width, change in the distance between the cuts along the length of the substrate, obtained from [15].

We can define the face angles as a function of strain with the following equations.

$$\theta = cos^{-1}\left(\frac{1}{\varepsilon A + 1}\right) \tag{3.1}$$

$$\beta = sin^{-1}\left(\frac{y}{Lc} tan\theta\right) \tag{3.2}$$

Furthermore, β can be expressed in terms of the cut ratio and **θ**, and $\boldsymbol{\rho}$ as follows.

$$\beta = sin^{-1}(\frac{2Rx}{RxRy-Ry}) \quad (3.3)$$

$$\rho=\cos-1(\cos\theta\cos\beta) \quad (3.4)$$

The graphs in Figures 3.2 through 3.4 illustrate the relationship between the face angles of incidence and the axial strain applied to the Kirigami model. Given the multiple angles that describe the geometry of the Kirigami structure, various graphs are plotted to capture these different aspects. These graphs demonstrate how each facet and leg of the model changes with varying cut ratios. Specifically, for the face angle of incidence, there is only one curve, indicating that cut ratios do not affect the value of θ.

The angles are crucial in this analysis because they influence the model's PCE and transmittance. Understanding these relationships is essential for predicting how different configurations will affect power generation, as the orientation and strain of the Kirigami structure can significantly impact its performance in practical applications.

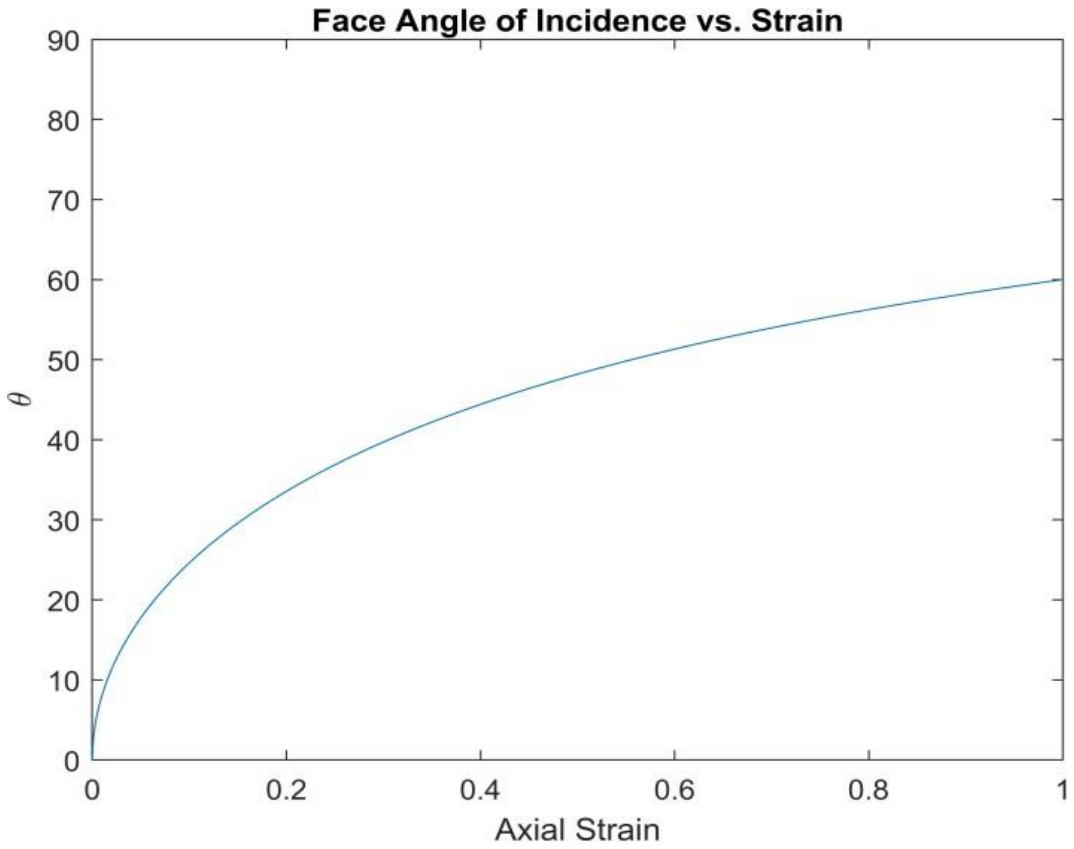

Figure 3.2. Graph showing the relation between Theta angle vs Strain for a uniaxially strained substrate obtained from MATLAB

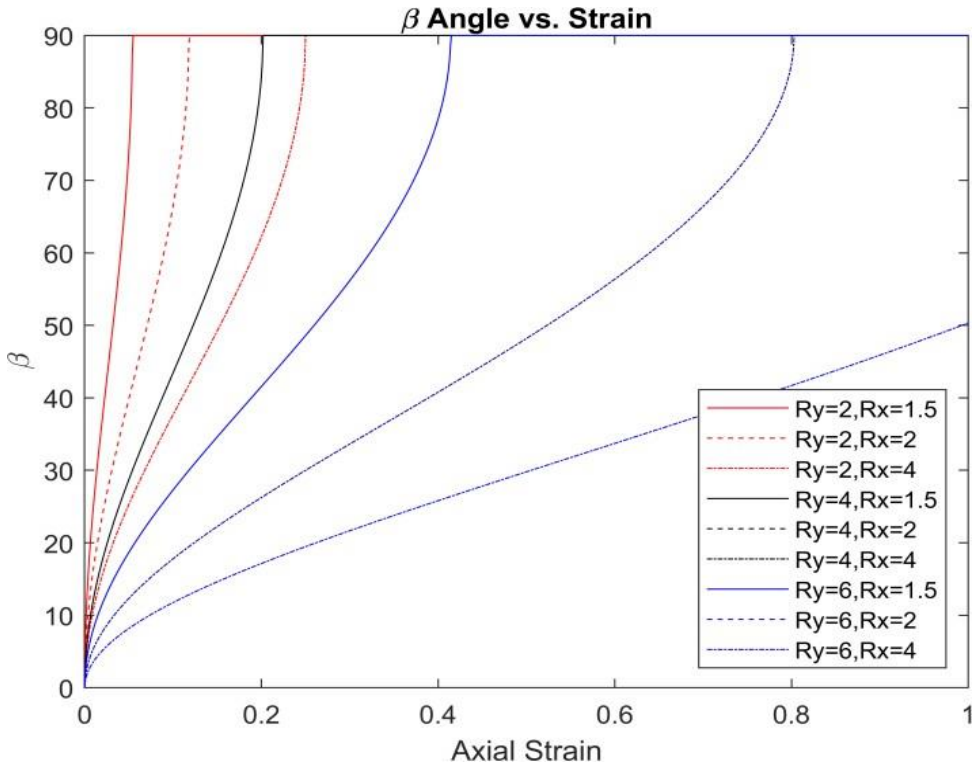

Figure 3.3. Graph showing the relation between Beta angle vs Strain for a uniaxially strained substrate obtained from MATLAB.

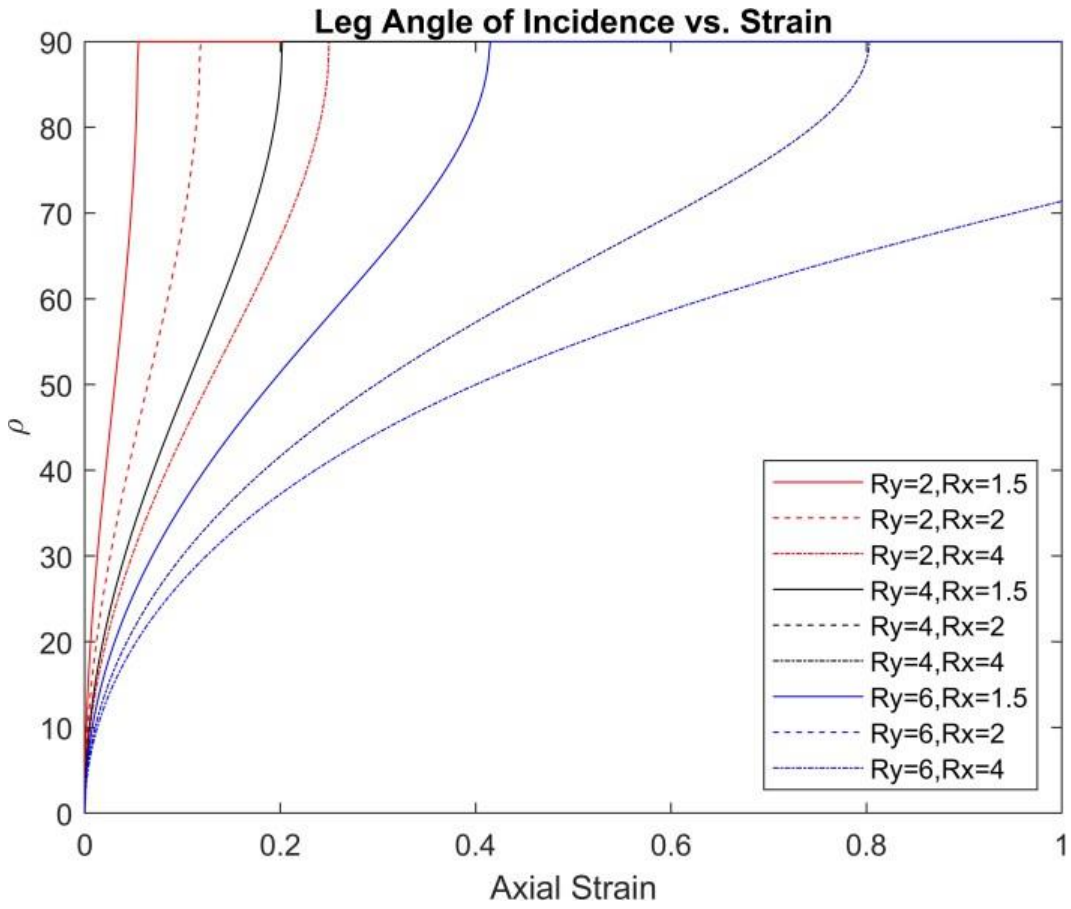

Figure 3.4. Graph showing the relation between Rho angle vs Strain for a uniaxially strained substrate obtained from MATLAB.

3.2. Power conversion efficiency

3.2.1. PCE vs Angles of Incidence

The angle at which incident light enters an OPV cell significantly affects its PCE. As the angle of incidence increases from zero (normal incidence), the PCE typically decreases from its maximum value. PCE doesn't start to drop off significantly until the angle of incidence approaches sixty degrees. After this, the PCE declines more precipitously. The model used to simulate the PCE versus the angle of incidence for OPVs employs a transfer matrix approach, which is a powerful method for analyzing the optical properties of multi-layer thin-film structures [13]. This method involves solving Maxwell's equations for the electric and magnetic fields across different layers, considering the complex refractive indices and thicknesses of each layer. The OPV cell is modeled as a stack of layers, including the transparent electrode, active layer (using PM6), buffer layers, and reflective back electrode. Each layer has specific refractive indices and thicknesses. For each layer, a transfer matrix is calculated, relating the electric fields at the layer's boundaries. The overall transfer matrix for the stack is obtained by multiplying the individual matrix. Key parameters include the phase shift in each layer and the characteristic impedance. Boundary conditions at each interface determine the incident, reflected, and transmitted fields, using Fresnel coefficients for reflection and transmission. These coefficients help calculate the reflectance and transmittance. The absorption in each layer is determined by the decrease in light intensity as it propagates through the material. From the absorption, it is assumed that one photon leads to exciton. The internal quantum efficiency (charge collection per photon absorbed) is assumed to be close to 100% for light absorbed above the organic semiconductor bandgap. This can be used to estimate the photocurrent generation. To get the PCE, the open circuit voltage and fill factor

of the solar cell are approximated based on experimental results [22]. The angle of incidence affects the path length and phase shift of light within each layer. As the angle increases from 0°, changes in interference patterns and electric field distribution within the layers occur. The simulation indicates that PCE is highest at normal incidence (0°) and decreases as the angle increases. This decrease is due to increased reflection and reduced absorption efficiency at oblique angles. The PCE with incident light angle for the PM6:Y6 system considered in this work is given in Figure 3. 5.

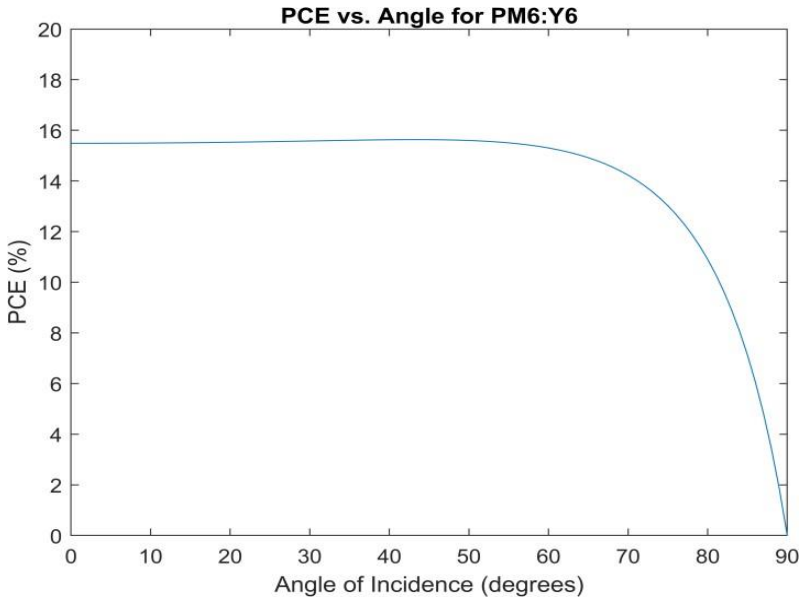

Figure 3.5. Graph showing the relation between Angle of Incidence vs PCE for a uniaxially strained substrate obtained from MATLAB.

3.2.2. Transmittance analysis

The transmittance of Kirigami-cut OPVs is dictated by the structural openness, which is controlled by the degree of strain applied to the Kirigami pattern. The Kirigami structure's initially flat facets tilt and split when force is applied, leaving spaces between the pattern's constituent pieces. Because of the increased openness, more light can flow through the structure as opposed to being absorbed. In Figure 3.7, we can see that the facets stay nearly in line at low strain (0% to 30%), which leaves few gaps and low transmission (usually less than 10%). The facets tilt more dramatically at moderate strains (30% to 60%), widening the gaps and increasing the amount of light that may pass through; transmittance values even rise to 40% at this point. The transmittance approaches 80% to 90% at high strain levels (60 to 90%) due to the facets' extreme tilt and gap maximization. The expanding gap size and the smaller effective absorption area together provide an exponential increase in transmittance with strain, highlighting the clear correlation between openness and the structure's capacity to transmit light. The correlation between transmittance and other factors, such as strain and PCE, may be comprehended by analyzing the impact of the Kirigami structure's tilt and strain on these metrics.

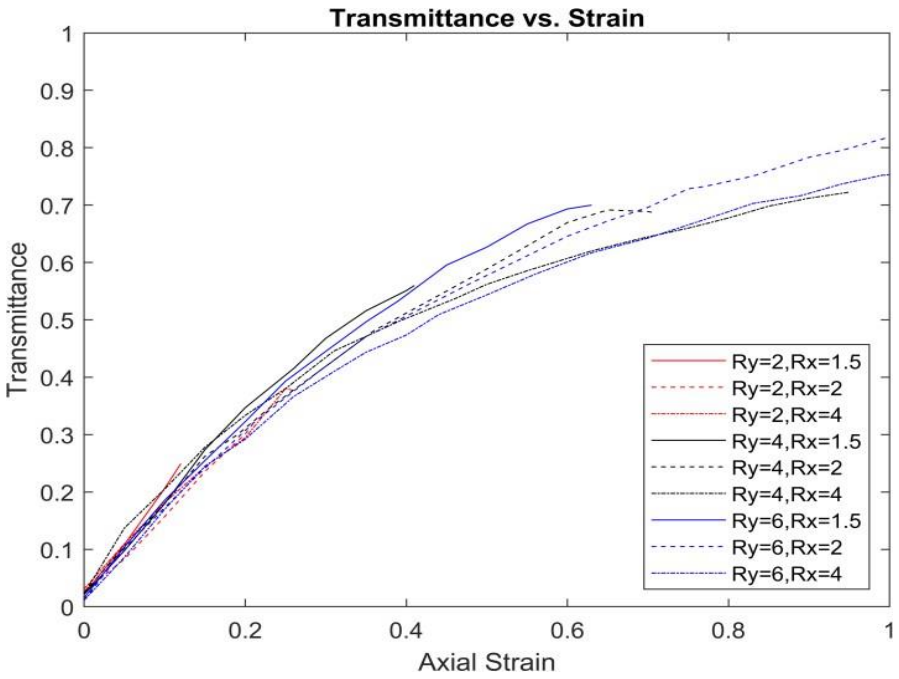

Figure 3.6. Graph showing the relation between Transmittance vs Strain for a uniaxially strained substrate obtained from MATLAB.

The impact of Rx and Ry was also individually studied. This was carried out to find out which cut ratio, either Rx or Ry, had a greater impact on the module. The wider variance in openness values along the top row of plots in Figure 3.7 illustrates how data analysis also showed that the Rx spacing of the cuts had a greater effect on the opening of the Kirigami than the Ry spacing. At lower Rx values, the Kirigami substrates open more quickly, while at higher Rx values, the maximum strains increase. The bottom row of Figure 3.7 shows that when Ry is changed, all of the plots overlap, demonstrating poor sensitivity to openness.

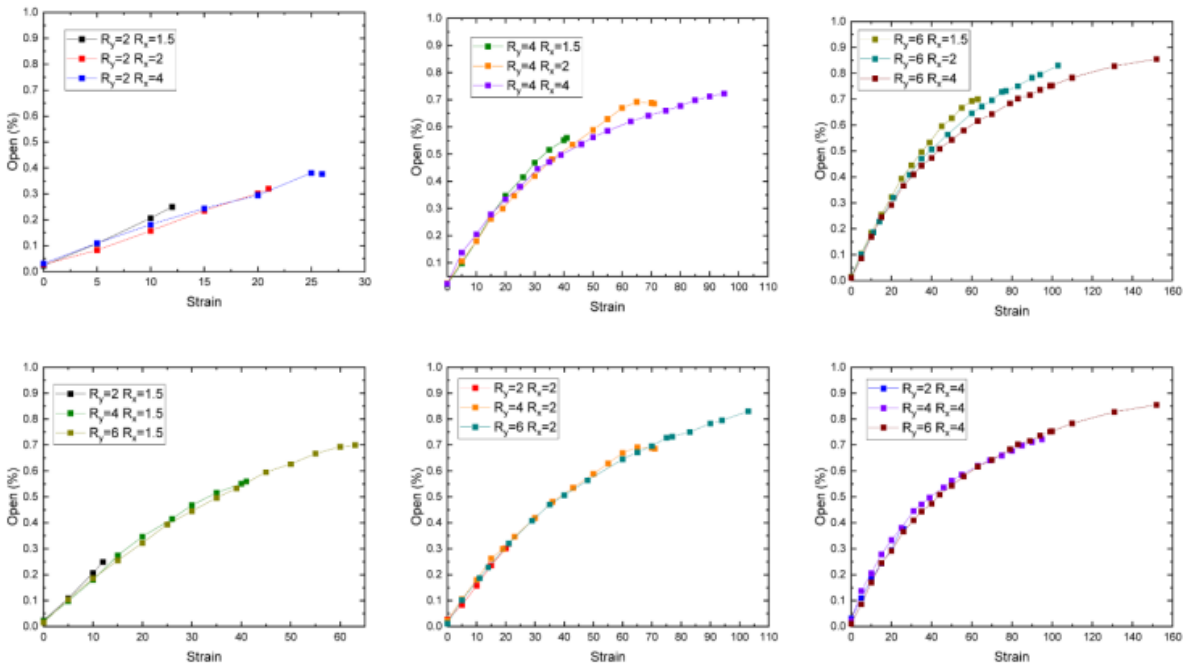

Figure 3.7. Openness vs Strain of Kirigami module with Ry held constant in the top row and Rx held constant in the bottom row.

3.2.3. Relation between transmittance and angle of incidence

In Kirigami-cut OPVs, the transmittance is also influenced by the incoming light's angle of incidence (θ). We recall that the angle at which light strikes the solar cell's surface concerning the perpendicular is known as the angle of incidence. The amount of light that may travel through the structure varies as the angle of incidence rises from 0 degrees when light strikes the surface perpendicularly. Light interacts with the surface directly at normal incidence (0 degrees), resulting in the greatest absorption and minimum transmission. Because of the Kirigami facets' tilt, the

effective area for light interaction diminishes with increasing angle, resulting in increased transmittance. Because transmittance and angle of incidence are inversely correlated, transmittance typically falls as the angle of incidence rises. This relationship results from more light being absorbed or reflected by the material at greater angles of incidence, which lowers the amount of light that passes through. For example, transmittance is usually maximum at a normal incidence angle of 0 degrees because light enters directly and is not greatly reflected. Because of increasing reflection, transmittance somewhat decreases when the angle rises to 30 degrees. As the route length through the material grows at 60 degrees, the reduction becomes more noticeable, improving both absorption and scattering.

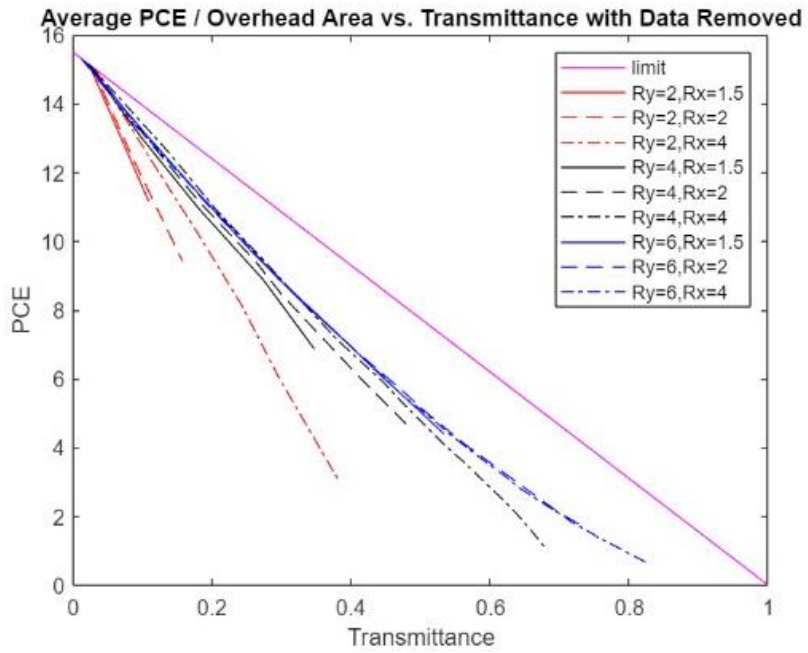

Figure 3.8. Graph showing the relation between Transmittance vs PCE for a uniaxially strained substrate obtained from MATLAB.

Transmittance can drastically decrease beyond 60 degrees, almost 90 degrees because most light is either absorbed by the substance or reflected off its surface. If transmittance is 100% at normal incidence (0 degrees), for example, for a given set of values, it may drop to 80-90% at 30 degrees, 50-70% at 60 degrees, and 10-30% as the angle gets closer to 90 degrees. The refractive index and surface characteristics of the material affect this trend.

3.2.4. Interrelation of Transmittance, PCE, and Strain

The facets of the structure tilt when strain is applied to the Kirigami design, resulting in bigger holes that let more light transmit. Because more light is transferred via the gaps rather than absorbed by the solar cell, the enhanced openness results in higher transmittance. On the other hand, the PCE reduces as a result of the tilting of the cells and larger gap size, which decreases the effective area accessible for light absorption. The angle of incidence on the slanted facets can be used to quantify the relationship between these characteristics. The Kirigami facets maintain their low transmittance and high PCE at low strain levels by staying comparatively flat. Both PCE and transmittance alter more dramatically as the strain rises to moderate levels; transmittance increases because the openness increases, while PCE starts to decrease.

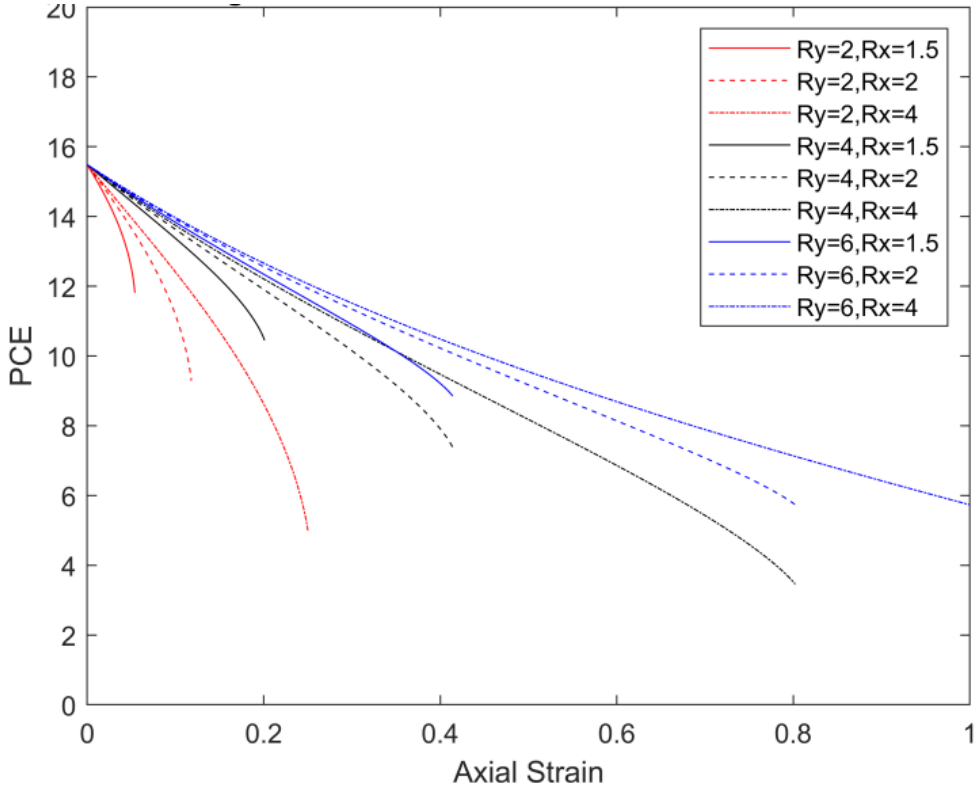

Figure 3.9. Graph showing the relation between PCE vs Strain for a uniaxially strained substrate obtained from MATLAB.

Because of the lesser light absorption area at high strain levels, the structure is highly open, resulting in maximum transmittance but a significant loss in PCE. To achieve the desired trade-off between high transmittance and acceptable PCE, this complex equilibrium requires rigorous strain adjustment. This is important for applications requiring flexible solar energy harvesting and dynamic light management. In the graph below, a sudden flattening of the curve is observed, this indicates the moment when the face of the panel has tilted such that the beta angle reaches 90 degrees and the Kirigami panel ceases to be in this physical state. At this point, there will be no power generated.

To understand the OPV performance characteristics better, we can calculate the LUE of all the modules using the transmittance and the PCE. LUE for different strain values is calculated as

the product of the transmittance and the PCE for each cut ratio. The ST-OPVs had a PCE of 7.14% and an AVT = 33%, based on literature. [23] The LUE values are plotted in Figure 3.9 for all the cut ratios except for Ry=2 since it had low openness and maximum strain values. The modules showed higher initial values for LUE at around 2.5, increasing to 2.75 at 20% strain. Then, the LUE decreases due to the reduction of PCE as the face shades itself. Based on the LUE values, we can see that Rx=2, Ry=4 was the best cut pattern.

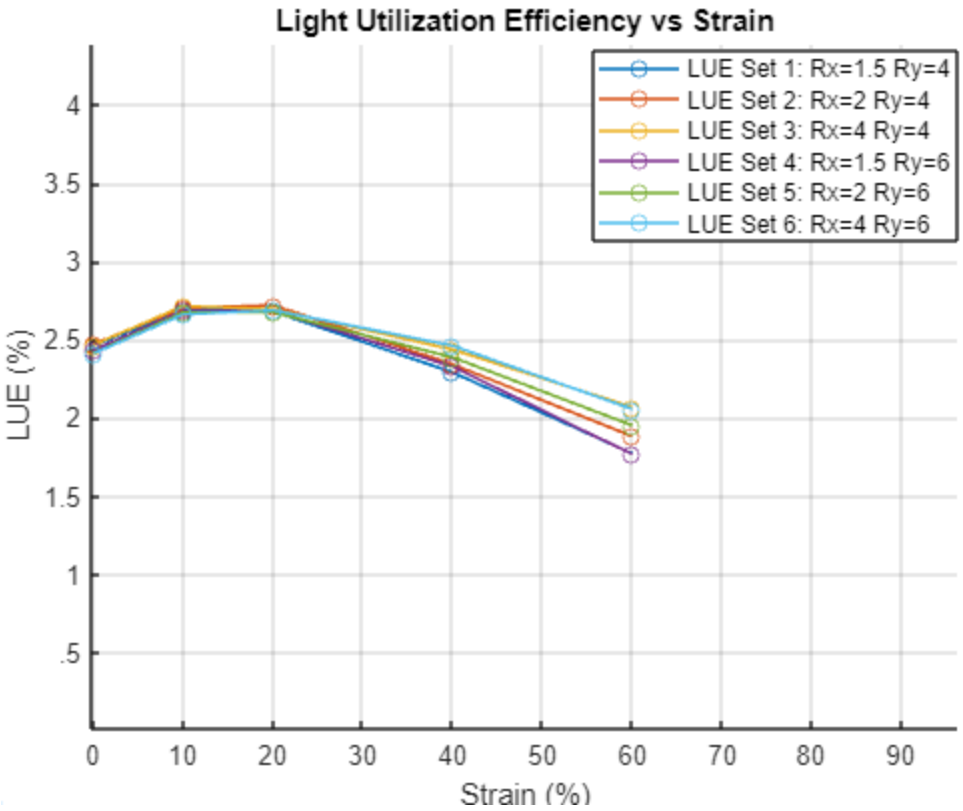

Figure 3.10. LUE for Kirigami cut patterns as a function of strain

Chapter 4: Conclusion

This study presents a novel approach to designing and optimizing Kirigami-patterned organic solar cells with tunable optical and electrical properties. The research methodology

involved creating parametric 3D models of parallel-cut Kirigami structures and using FEA to simulate their mechanical behavior under strain. By combining these structural simulations with optical modeling and analytical geometry analysis, the study predicted both transmittance and PCE as functions of applied strain and cut pattern design.

The integrated modeling approach allowed for the exploration of a wide design space and identification of optimal configurations for different applications.

The performance and openness of the Kirigami structures can be inferred by altering the cut ratios Rx and Ry while maintaining a fixed cut length of 6 cm. The open area percentage grew significantly as the Rx values were raised from 1.5 to 4, with the largest open area recorded at Rx being 4. Furthermore, an increased open area was obtained by adjusting Ry from 2 to 6 for each Rx value, indicating that both cut ratios have a favorable impact on structural openness. Larger distances between cuts along both axes promote openness; the combination of Ry being 6 and Rx being 4 produced the most open area at 55%.

For solar cells made of origami, the ideal values of Rx and Ry depend on how best to balance transmittance and PCE. Lower Rx and Ry values are better for high-efficiency solar farms because they reduce openness and improve direct light absorption, which maximizes PCE. Higher Rx and Ry values, on the other hand, promote openness, which is advantageous for applications needing greater transmittance, including greenhouses and semitransparent solar windows. In building-integrated photovoltaics (BIPV), where both energy generation and light passage are crucial, intermediate values of Rx and Ry strike a balance between PCE and transmittance. To maximize the performance of Kirigami-cut solar cells in a variety of applications, these relationships are essential.

In conclusion, the efficiency and light transmission properties of solar cells based on origami are greatly influenced by the selection of Rx and Ry values. It is feasible to customize the solar cells for particular uses, such as optimizing energy output, improving light transmittance, or striking a balance between the two, by carefully choosing these variables. Modern solar energy systems can benefit from a flexible and effective solution provided by Kirigami structures, which

allow for the dynamic adjustment of the openness and angle of incidence. Because of their versatility, Kirigami solar cells hold great promise for a range of uses, including creative building integration and highly efficient solar farms, all of which will further the development of renewable energy technologies.

The Kirigami models' structural integrity held up despite their increased openness, which made them appropriate for uses like flexible solar panels and adaptive shading devices that demand excellent light transmittance and flexibility. The study emphasizes how crucial it is to optimize cut ratios to strike the ideal compromise between structural performance and openness.

Chapter 5: References

[1] C.-Y. Tsai, Y.-H. Lin, Y.-M. Chang, J.-C. Kao, Y.-C. Liang, C.-C. Liu, J. Qiu, L. Wu, C.-Y. Liao, H.-S. Tan, C. Yu-Chiang, S.-F. Horng, H.-W. Zan, H.-F. Meng and F. Li, "Large area organic photovoltaic modules fabricated on a 30 cm by 20 cm substrate with a power conversion efficiency of 9.5%," *Solar Energy Materials and Solar Cells,* vol. 218, no. 0927-0248, 2020.

[2] F. Dimroth, M. Grave, P. Beutel, U. Fiedeler, C. Karcher, T. N. Tibbits, E. Olivia, G. Siefer, M. Schachtner, A. Wekkeli, A. W. Bett, R. Krause, M. Piccin, N. Blanc, C. Drazek, E. Guiot, B. Ghyselen, T. Salvetat, A. Tauzin, T. Signamarcheix, A. Dobrich, T. Hannappel and K. Schwarzburg, "Wafer bonded four-junction GaInP/GaAs//GaInAsP/GaInAs concentrator solar cells with 44.7% efficiency," *Progress in Photovoltaics,* vol. 22, no. 3, pp. 277-282, 2014.

[3] A. S. Bati, Y. L. Zhong, P. L. Burn, M. K. Nazeeruddin, P. E. Shaw and M. Batmunkh, "Next-generation applications for integrated perovskite solar cells," *Communications Materials,* vol. 4, no. 1, 2022.

[4] G. Bernardo, T. Lopes, D. G. Lidzey and A. Mendes, "Progress in Upscaling Organic Photovoltaic Devices," *Advanced Energy Materials,* vol. 11, no. 2100342, 30 April 2021.

[5] E. K. Solak and E. Irmal, "Advances in organic photovoltaic cells: a comprehensive review of materials, technologies, and performance," *RSC advances,* vol. 13(18), no. 12244–12269, 2023.

[6] Y. Li, W. Huang, D. Zhao, L. Wang, Z. Jiao, Q. Huang, P. Wang, M. Sun and G. Yuan, "Recent Progress in Organic Solar Cells: A Review on Materials from Acceptor to Donor," *Molecules,* vol. 27, no. 6, p. 1800, 2022.

[7] F. C. Krebs, "Fabrication and processing of polymer solar cells: A review of printing and coating techniques," *Solar Energy Materials and Solar Cells,* vol. 93, no. 4, pp. 394-412, 2009.

[8] H. Iftikhar, G. G. Sonai, S. G. Hashmi, A. F. Nogueira and P. D. Lund, "Progress on Electrolytes Development in Dye-Sensitized Solar Cells," *Materials,* vol. 12, no. 12, 2019.

[9] Y. Zhao, G. A. Meek, B. G. Levine and R. R. Lunt, "Near-Infrared Harvesting Transparent Luminescent Solar Concentrators," *Advanced Optical Materials,* vol. 2, no. 7, pp. 606-611, 2014.

[10] P. Sonar, J. P. F. Lim and K. L. Chan, "Organic non-fullerene acceptors for organic photovoltaics," *Energy & Environmental Science,* vol. 4, no. 5, pp. 1558-1574, 2011.

[11] W. Gao, Y. Zhang, D. Ramanujan, K. Ramani, Y. Chen, C. B. Williams, C. C. Wang, Y. C. Shin, S. Zhang and P. D. Zavattieri, "The status, challenges, and future of additive manufacturing in engineering," *Computer-Aided Design,* vol. 69, no. 0010-4485, 2015.

[12] S. M. Felton, M. T. Tolley, B. Shin, C. D. Onal, E. D. Demaine, D. Rus and R. J. Wood, "Self-folding with shape memory composites," *Soft Matter,* vol. 9, no. 32, 2013.

[13] L. Pettersson, L. S. Roman and O. Inganas, "Modeling photocurrent action spectra of photovoltaic devices based on organic thin films," *Journal of Applied Physics,* vol. 86, 1999.

[14] N. Yeh and P. Yeh, "Organic solar cells: Their developments and potentials," *Renewable and Sustainable Energy Reviews,* vol. 21, pp. 421-431, 2013.

[15] A. Lamoureux, K. Lee, M. Shlian, S. R. Forrest and M. Shtein, "Dynamic Kirigami structures for integrated solar tracking," *Nature Communications,* vol. 6, no. 1, Sep 2015.

[16] T. U. Lee, J. M. Gattas and Y. M. Xie, "Bending-active Kirigami," *International Journal of Solids and Structures,* vol. 254–255, no. 0020-7683, 2022.

[17] Y. Sun, W. Ye, Y. chen, W. Fan, J. Feng and P. Sareh, "Geometric design classification of Kirigami-inspired metastructures and metamaterials," *Structures,* vol. 33, no. 2352-0124, pp. 3633-3643, 2021.

[18] R. Xu, A. Zverev, A. Hung, C. Shen, L. Irie, G. Ding, M. Whitmeyer, L. Ren, B. Griffin, J. Melcher, L. Zheng, X. Zang, M. Sanghadasa and L. Lin, "Kirigami-inspired, highly stretchable micro-supercapacitor patches fabricated by laser conversion and cutting," *Microsystems & Nanoengineering,* vol. 4, no. 1, pp. 661-664, 2018.

[19] A. Rafsanjani and K. Bertoldi, "Buckling-Induced Kirigami," *Physical Review Letters,* vol. 118, no. 8, p. 084301, 2017.

[20] J. Tao, H. Khosravi, V. Deshpande and S. Li, "Engineering by Cuts: How Kirigami principle enables unique mechanical properties and functionalities," *Advanced Science,* vol. 10, no. 1, Oct 2022.

[21] Y.-G. Kim, J.-H. Song, S. Hong and S.-H. Ahn, "Piezoelectric strain sensor with high sensitivity and high," *npj Flexible Electronics,* vol. 6, no. 1, p. 52, 2022.

[22] W. Shockley and H. J. Queisser, "Detailed Balance Limit of Efficiency of p-n Junction Solar Cells," *Journal of Applied Physics,* vol. 32, no. 3, 1 March 1961.

[23] Y. Xiong, R. E. Booth, T. Kim, L. Ye, Y. Liu, M. Zhang, Q. Dong, F. So, Y. Zhu, A. Amassian, B. T. O'Connor and H. Ade, "Novel bimodal silver nanowire

network as top electrodes for reproducible and High-Efficiency semitransparent organic photovoltaics," *Solar RRL*, vol. vol. 4, no. 10, p. 9, Aug 2020.

[24] Q, Liu, et al., "18% Efficiency organic solar cells," *Science Bulletin*, p. 272–275, Feb 2020.

[25] M. Noman, Z. Khan and S. T. Jan, "A comprehensive review on the advancements and challenges in perovskite solar cell technology," *RSC Advances*, p. 5085–5131, Jan 2024.

[26] R. M and L. S, "A method to attain power optimality and efficiency in solar panel," *Beni-Seuf University Journal of Basic and Applied Sciences /Beni-Suef University Journal of Basic and Applied Sciences*, vol. 7, no. 4, p. 705–708, Dec 2018.

[27] S. Gorjian, F. Calise, K. Kant, M. S. ahamed, B. copertaro, G. Najafi, X. Zhang, M. Aghaei and R. R. Shamshiri, "A review on opportunities for implementation of solar energy technologies in agricultural greenhouses," *Journal of Cleaner Production*, vol. 285, no. 0959-6526, 2021.

[28] R. H. E. Hassanien, M. Li and W. D. Lin, "Advanced applications of solar energy in agricultural greenhouses," *Renewable & sustainable energy reviews*, p. 54, Feb 2016.

[29] T.-S. Zhan, L. Whei-Min, M.-H. Tsai and G.-S. Wang, "Design and implementation of a Dual-Axis solar tracking System," *Energies*, vol. 16, no. 17, Aug 2023.

[30] D. H. LI, T. N. Lam, W. W. Chan and A. H. Mak, "Energy and cost analysis of semi-transparent photovoltaic in office buildings," *Applied Energy*, vol. 86, no. 5, pp. 722-729, May 2009.

[31] Y. Nagatomo, A. Ozawa, Y. Kudoh and H. Hondo, "Impacts of employment in power generation on renewable-based energy systems in Japan— Analysis using an energy system model," *Energy*, July 2021.

[32] C. Candelise, M. Winskel and R. Gross, "Implications for CdTe and CIGS technologies production costs of indium and tellurium scarcity," *Progress in Photovoltaics*, vol. 20, no. 6, p. 816–831, Jun 2012.

[33] N. S. Sariciftci and H. Hoppe, "Organic solar cells: An overview," *Journal of Materials Research/Pratt's Guide to Venture Capital Sources,* vol. 19, no. 7, p. 1924–1945, Jul 2004.

[34] P. Romero-Gómez, F. Pastorelli, P. Mantilla-Pérez, M. Mariano, A. Martínez-Otero, X. Elias, R. Betancur and J. Martorell, "Semi-transparent polymer solar cells," *Journal of Photonics for Energy*, vol. 5, no. 1, Feb 2015.

[35] E. Kabir, P. Kumar, S. Kumar, A. A. Adelodun and K.-H. Kim, "Solar energy: Potential and future prospects," *Sustainable Energy Reviews*, vol. 82, pp. 894-900, Feb 2018.

[36] A. Pospischil, M. M. Furchi and T. Mueller, "Solar-energy conversion and light emission in an atomic monolayer p–n diode," *Nature Nanotechnology*, vol. 9, no. 4, p. 257–261, Mar 2014.

[37] A. Firouzeh, T. Higashisaka, . K. Nagato, K. Cho and J. Paik, "Stretchable Kirigami components for composite Meso-Scale robots," *IEEE Robotics & Automation Letters*, vol. 5, no. 2, p. 1883–1890, Apr 2020.

[38] E. Fortunato, D. Ginley, H. Hosono and D. C. Paine, "Transparent conducting oxides for photovoltaics," *MRS Bulletin*, vol. 32, no. 3, p. 242–247, Mar 2007.